Global Change Biology (2003) **9,** 1241–1250

Simulated variations in atmospheric CO_2 over a Wisconsin forest using a coupled ecosystem–atmosphere model

A. SCOTT DENNING*, MELVILLE NICHOLLS*, LARA PRIHODKO*, IAN BAKER*, PIER-LUIGI VIDALE†, KENNETH DAVIS§ and PETER BAKWIN¶

**Department of Atmospheric Science, Colorado State University, Fort Collins, CO 80523-1371, USA, †Institute for Atmospheric and Climate Science, ETH Zurich, Switzerland, §Department of Meteorology, The Pennsylvania State University, University Park, PA 16802-5013, USA, ¶Climate Monitoring and Diagnostics Laboratory, NOAA/OAR, R/CMDL1, Boulder, CO 80303, USA*

Abstract

Ecosystem fluxes of energy, water, and CO_2 result in spatial and temporal variations in atmospheric properties. In principle, these variations can be used to quantify the fluxes through inverse modelling of atmospheric transport, and can improve the understanding of processes and falsifiability of models. We investigated the influence of ecosystem fluxes on atmospheric CO_2 in the vicinity of the WLEF-TV tower in Wisconsin using an ecophysiological model (Simple Biosphere, SiB2) coupled to an atmospheric model (Regional Atmospheric Modelling System). Model parameters were specified from satellite imagery and soil texture data. In a companion paper, simulated fluxes in the immediate tower vicinity have been compared to eddy covariance fluxes measured at the tower, with meteorology specified from tower sensors. Results were encouraging with respect to the ability of the model to capture observed diurnal cycles of fluxes. Here, the effects of fluxes in the tower footprint were also investigated by coupling SiB2 to a high-resolution atmospheric simulation, so that the model physiology could affect the meteorological environment. These experiments were successful in reproducing observed fluxes and concentration gradients during the day and at night, but revealed problems during transitions at sunrise and sunset that appear to be related to the canopy radiation parameterization in SiB2.

Keywords: atmosphere–biosphere interactions, large eddy simulation, mesoscale modelling, net ecosystem exchange

Received 15 April 2002; revised version received and accepted 16 April 2002

Introduction

The global carbon budget has been studied in terms of both local measurements and modelling of the processes involved, and in terms of the effects of these processes at hemispheric and global scales. The process-based studies are crucial to understanding and predicting changes in the global carbon cycle that affect the concentration of atmospheric CO_2, but the representativeness of any given field study is difficult or impossible to assess. A significant challenge to the interpretation of local studies is to extrapolate their results to regional, continental, and global scales, from the 'bottom-up'. Conversely, global inverse calculations of the carbon budget have the advantage of providing quantitative information about the integrated effects of physical, biogeochemical, and anthropogenic processes over huge spatial areas. These 'top-down' studies provide a spatially integrated 'snapshot' of the current state of the carbon cycle, but can provide little information about the processes responsible or how these might change in the future. Inverse methods are able to provide robust estimates of fluxes only at the largest spatial scales: global and hemispheric annual means are well constrained, but different transport models or inverse methods produce very different estimates of even continental fluxes on a monthly basis (e.g. Fan *et al.*, 1998; Rayner *el al.*, 1999; Gurney *et al.*, 2002). The challenge to inverse modellers is to refine the resolution of their calculations to the point that they can provide a meaningful integral constraint for the 'bottom-up' studies of processes.

Correspondence: A. Scott Denning, fax +1 970 491 8449, e-mail: denning@atmos.colostate.edu

Very few studies have addressed the gap in spatial scales between whole-ecosystem studies of long-term carbon flux by eddy covariance (with a 'footprint' of perhaps 1 km^2) and time-dependent tracer transport inversions (which are difficult to interpret over areas much smaller than 10^8 km^2). This huge spatial gap was identified as a priority for future data collection in a recent set of recommendations for carbon cycle research (Sarmiento *et al.*, 1999), but the design of mesoscale observing systems will require preliminary studies of the variability of CO_2 and other relevant tracers to be effective.

Mesoscale studies of atmosphere–biosphere exchanges of heat, water, momentum, and CO_2 can also provide an opportunity to test process-based models in new ways. Land–atmosphere interactions occur on a wide range of scales: local energy and water fluxes influence temperatures and humidity; heterogeneity of vegetation and land use at larger scales can result in systematic atmospheric circulations and changes in cloudiness and precipitation (e.g. Charney *et al.*, 1975; Shukla & Mintz, 1982; Avissar & Pielke, 1991; see the review by Pielke *et al.*, 1998). Ecophysiological models have long been tested against point measurements at tower sites, but the spatial scaling of these processes to larger regions is difficult to test. The data record collected over 6 years at the WLEF-TV tower in Wisconsin provides an opportunity to test such scaling in land–atmosphere models, because of its ability to sample above the immediate surface layer environment of the forest below (Bakwin *et al.*, 1998). The flux footprint of the tower expands with height, to cover many kilometres at the top of the tower. The concentration record, however, records the influence of much larger areas upwind, responding to fluxes encountered by air masses which travelled for hundreds of kilometres before reaching the tower.

The atmospheric model employed in this study is applicable to a wide range of spatial scales, from the mesoscale (tens to hundreds of kilometres) down to the small-scale turbulent eddies occurring in the atmospheric boundary layer. Here we test the coupled ecophysiological–atmospheric modelling system, by running it in two-dimensional (x–z) mode, simulating vertical and along-wind variations. These experiments are quite different from the common practice of 'forcing' an ecophysiology model with observed weather. In the fully coupled simulations reported here, the weather and ecosystems interact. The behaviour of both the atmosphere and the ecosystems is predicted by the model, with only initial conditions in both components being specified. Results of a high-resolution simulation are compared with observations made for a 2-day period, at the WLEF-TV tower. Canopy and soil parameters for the ecophysiology model are specified from satellite imagery and a database of soil textural properties (Sellers *et al.*, 1996b; Los *et al.*, 2000). The ecophysiology model was tested at the scale of the immediate flux footprint for 3 years (1997–1999), and found to be reasonably successful in capturing fluxes of heat, moisture, and CO_2 over diurnal and synoptic timescales (Baker *et al.*, this issue). This paper presents first results from experiments with a coupled mesoscale model of forest–atmosphere interactions in the vicinity of the WLEF tower.

Methods

The WLEF-TV tower site

The Wisconsin forest site is the location of a 450 m tall television transmission tower (WLEF-TV, 45°55′-N, 90°10′-W), located in the Chequamegon National Forest, 24 km west of Park Falls, WI. The region is in a heavily forested zone of low relief. The region immediately surrounding the tower is dominated by boreal lowland and wetland forests typical of the region. Much of the area was logged, mainly for pine, during 1860–1920, and has since re-grown. The concentration of CO_2 has been measured continuously at six heights (11, 30, 76, 122, 244, and 396 m above the ground) since October 1994, and CO_2 flux has been measured at three heights at this tower (30, 122, and 396 m) since 1996. Micrometeorology and soil temperature and moisture data are collected at the site or at the nearby USDA Forest Sciences Laboratory. Another significant advantage of this site is that the great height of the tower provides the opportunity for observing the carbon balance over a 'footprint' that increases with height on the tower up to several square kilometers for the highest observing platform, which is approximately two orders of magnitude greater than other Ameriflux monitoring sites.

Model descriptions

The Simple Biosphere (SiB) Model, developed by Sellers *et al.* (1986), has undergone substantial modification (Sellers *et al.*, 1996a, b), and is now referred to as SiB2. The number of biome-specific parameters has been reduced, and most are now derived directly from processed satellite data rather than prescribed from the literature. The vegetation canopy has been reduced to a single layer. Another major change is in the parameterization of stomatal and canopy conductance used in the calculation of the surface energy budget over land. This parameterization involves the direct calculation of the rate of carbon assimilation by photosynthesis, making

possible the calculation of CO_2 exchange between the global atmosphere and the terrestrial biota on a time-step of several minutes (Denning *et al*., 1996a, b; Schaefer *et al*., 2002). Photosynthetic carbon assimilation is linked to stomatal conductance and thence to the surface energy budget and atmospheric climate by the Ball–Berry equation (Ball, 1988; Collatz *et al*., 1991, 1992; Sellers *et al*., 1992, 1996a).

Model parameters for SiB2 were specified from AVHRR imagery and soil texture data following the methods of Sellers *et al.* (1996b) and Los *et al.* (2000). Boundary conditions for SiB2 characterize land surface conditions at a location using a combination of land cover type (Hansen *et al*., 2000), monthly maximum normalized difference vegetation index (NDVI) derived from advanced very high-resolution radiometer (AVHRR) data (Teillet *et al*., 2000), and soil properties (Soil Survey Staff, 1994). Time-invariant biophysical parameters include quantities such as canopy height, leaf angle distribution, leaf transmittance, and parameters related to photosynthesis as well as soil hydraulic and thermal properties. Time-varying biophysical parameters include quantities such as leaf area index, fractional absorbed photosynthetically active radiation, and surface roughness length. Simulated variations in fluxes of energy, water, and carbon using SiB2 driven by observed meteorology for the site have been compared with observations by Baker *et al.* (this issue). Multiyear simulations driven by site meteorology were used to specify initial conditions (e.g. soil moisture and temperature) for SiB2 in the simulations described below.

The Regional Atmospheric Modelling System (RAMS) was developed at Colorado State University in order to facilitate the research of predominantly mesoscale and cloud-scale phenomena (Pielke, 1974; Tripoli & Cotton, 1982; Pielke *et al*., 1992; Nicholls *et al*., 1995; Nicholls & Pielke, 2000). The model solves the equations of motion, radiative transfer, and thermodynamics for a region of the atmosphere. A significant feature is the incorporation of a telescoping nested-grid capability (Walko *et al*., 1995a), which enables the simulation of phenomena involving a wide range of spatial scales. The model has been applied to the simulation of flows at scales as small as buildings (Nicholls *et al*., 1993, 1995) and so is aptly suited for studying the interactions between the atmosphere and terrestrial ecosystems, which take place at many spatial scales. The RAMS is a non-hydrostatic model and contains time-dependent equations for velocity, non-dimensional pressure perturbation, ice–liquid water potential temperature (see Tripoli & Cotton, 1981), total water mixing ratio, and cloud microphysics. Vapour mixing ratio and potential temperature are diagnostic. The model is compressible, permitting the propagation of sound waves. The turbulence closure scheme of Deardorff (1980) was used in this study, which employs a prognostic sub-grid turbulent kinetic energy. Lateral boundary conditions for all model variables were periodic, meaning that any property advecting out of the downwind boundary was immediately advected back into the upwind boundary. The two-stream radiation scheme developed by Harrington (1997) was used. Surface fluxes at the lower boundary were computed by SiB2.

The lowest level above the surface in the RAMS model is the reference level at which atmospheric boundary layer values of temperature, vapour pressure, wind velocity, and carbon dioxide partial pressure are provided as upper boundary conditions to SiB2. Additionally, the direct and diffuse components of shortwave and neat-infrared radiation incident at the surface are provided from the RAMS radiation scheme. The surface layer, which is between the surface and the reference level, is incorporated as part of the SiB2 model and is based on the scheme of Holtslag & Boville (1993). The input variables provided by RAMS to SiB2 are updated every 60 s of simulation time, and SiB2 provides back to RAMS, at the reference level, fluxes of radiations, heat, moisture, momentum, and carbon dioxide.

To investigate detailed processes in the immediate vicinity of the tower, we performed a high-resolution two-dimensional (x–z) simulation on the 26th and 27th of July 1997. The SiB2 parameters derived at the WLEF site (Baker *et al.* this issue) were used, without any tuning to the specific field site. The atmosphere was initialized from horizontally homogeneous vertical profiles of temperature, moisture, and wind, which were obtained by isentropic analysis from NCAR-NCEP reanalysis (Kalnay *et al*., 1996) at 06:00 hours on the 26th. A horizontal grid increment of 100 m was used and the vertical grid increment at the surface was 20 m, which was gradually stretched with height to the top of the domain. The domain width was 8 km and the height was 7 km, roughly the extent of the flux footprint at the top of the tower in moderately turbulent conditions. Simulations were carried out both with and without the cloud microphysics scheme activated. The RAMS microphysics scheme (Walko *et al*., 1995b) includes both the liquid and ice phases of water substance. For the period of this study, the clouds were scattered shallow cumulus composed of liquid water. The microphysics scheme has two categories of liquid water: (1) cloud water droplets, which advect with air parcels, and (2) rain water droplets, which are larger and are allowed to fall relative to air parcels. The cloud water droplets are mono-dispersed and the cloud

condensation nuclei were set to 1000 cm^{-3}, typical of continental air masses. A Marshall–Palmer distribution was employed for rain water droplets with a mean mass diameter of 1 mm. For the shallow cumulus clouds simulated in this study, most of the liquid water content remained in the cloud water category. The purpose of these simulations was to provide a realistic simulation of the small-scale structure and processes occurring at the WLEF site. Of course, since the domain was periodic, it did not include large-scale advective influences. Times cited are local standard time, and elapsed times are since midnight GMT (06:00 hours LST) on July 26, 1997.

Results and discussion

Although we chose to simulate a relatively simple case with minimal cloud cover and no precipitation, occasional shallow cumulus clouds were present during the experiment. Solar radiation input to the forest varied with the passing of these clouds (Fig. 1). The simulation with clouds is not intended to reproduce the detailed occurrence of these variations, but rather to introduce a realistic degree of variance in radiative forcing to the forest ecosystem. Modelled clouds reduced both the direct and diffuse shortwave radiation at the canopy top, and increased the diffuse fraction. Heating rates in SiB2 are computed using a two-stream radiation scheme that explicitly treats direct and diffuse radiation in both the visible and near infrared, but photosynthesis calculations treat only direct beam light extinction within the canopy. Therefore, the simulated physiological response to the changing ratio of direct to diffuse light was not realistic in either simulation. The simulated downward shortwave radiation in the cloud-free simulation was too smooth in time and somewhat too bright on average compared with the observations. The simulation including clouds captured the mean radiative forcing better, and also the variability associated with passing clouds. The simulated clouds did not arrive at the observed times, which is not surprising given the unpredictable nature of atmospheric turbulence. Also, passing clouds in the model absorbed much more radiation than is suggested by the observations. This results from the parameterization of cloud–radiation interactions in RAMS, which treats the phenomenon as a one-dimensional radiative transfer problem. Fully three-dimensional scattering and transfer of diffuse light from clear areas of sky that are not immediately overhead deliver much more radiation to the real forest under conditions of scattered cloud than was simulated by the model.

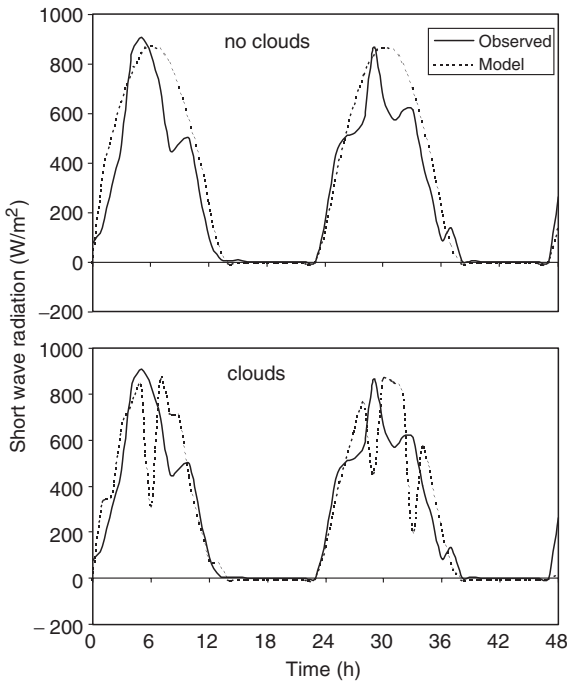

Fig. 1 Simulated and observed downward solar radiation for July 26–27, 1997. Simulations used the high-resolution, two-dimensional grid. The upper panel is for cloudless conditions, and the lower panel shows results including passing clouds. Time is elapsed hours since the beginning of the experiment at 06:00 hours LST on July 26, 1997.

Observed sensible heat flux (from eddy covariance measurements at the tower) is compared to the high-resolution two-dimensional simulations in Fig. 2. The model tends to overestimate the magnitude of the sensible heat flux relative to the observations, during both day and night. The time-mean sensible heat flux was better simulated when the effects of clouds were included, which is consistent with the results for radiative forcing. Variability in sensible heat flux associated with changes in radiative inputs due to passing clouds was present in both the cloudy simulation and observations, although the magnitude of these changes was exaggerated in the model. Both simulations exhibited stronger latent heat flux than observed (Fig. 3), and even the simulation with clouds underestimated the observed variability. The sum of sensible and latent heat flux simulated by the model exceeded the observed sum by almost 10 $W m^{-2}$ at mid-day. Given that the total incoming solar radiation was approximately correct, this 'extra' energy is likely due to a combination of underestimation of both albedo and soil thermal conductivity in the model (Baker *et al.*, this issue) and underestimation by the eddy covariance system (Davis *et al.*, this issue).

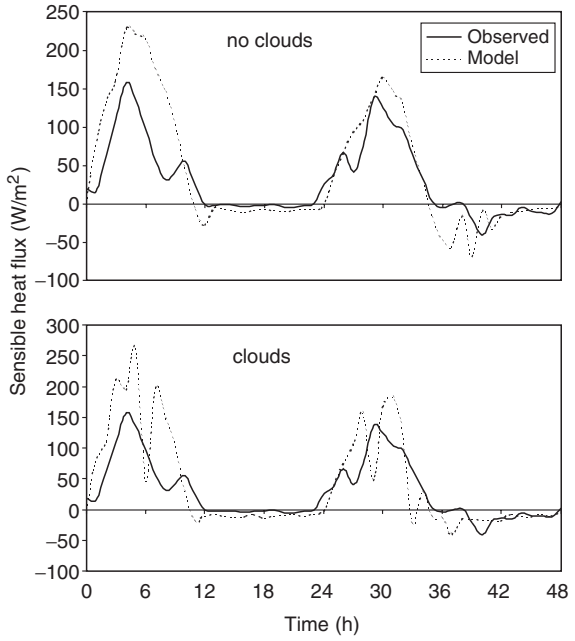

Fig. 2 Simulated and observed sensible heat fluxes for July 26–27, 1997, at 30 m. The upper panel is for cloudless conditions, and the lower panel shows results including passing clouds. Time is elapsed hours since the beginning of the experiment at 06:00 hours. LST on July 26, 1997.

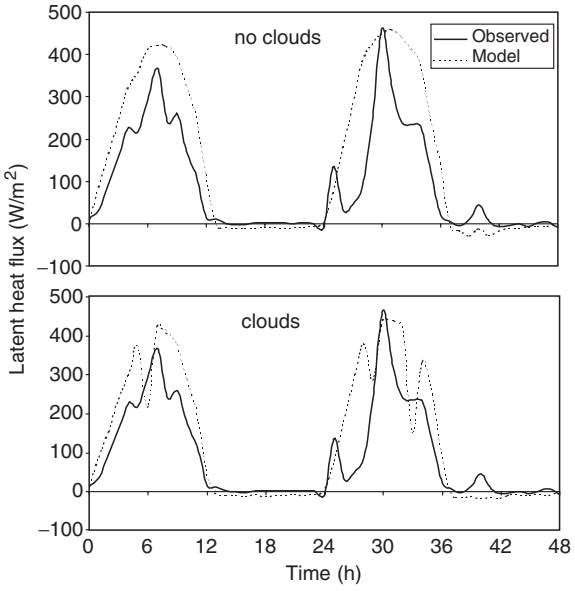

Fig. 3 As in Fig. 2, but for latent heat flux.

Net CO_2 flux to the atmosphere was reasonably well-simulated (Fig. 4). The observations were characterized by very weak fluxes at night, followed by a 'flush' of stored CO_2 as the stable layer broke up in the early

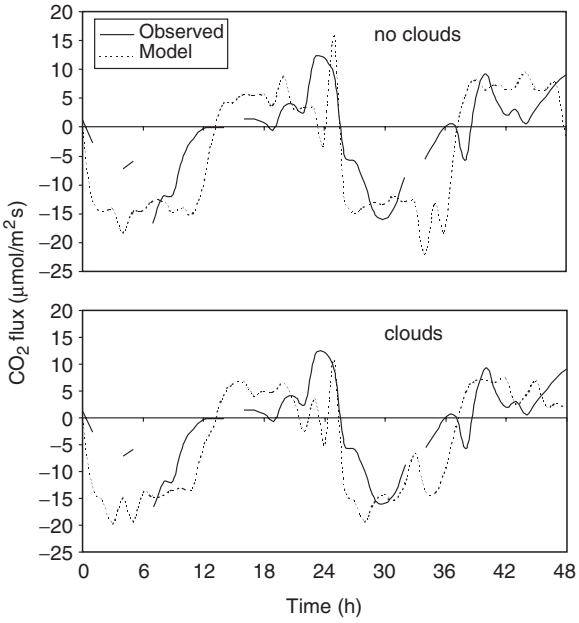

Fig. 4 As in Fig. 2, but for CO_2 flux.

morning. This phenomenon was also simulated by the model, although night-time respiration fluxes were stronger in the model than in the observations. This may reflect underestimation by the eddy covariance system under stable nocturnal conditions. Net uptake at mid-day was well-simulated, although the cloud-free simulation included the development of physiological stress in the middle of the second day, reducing net uptake by about 20% from 26 to 32 elapsed hours (10:00–16:00 hours July 27). Stomatal closure was much less pronounced in the simulation with clouds, because the overall radiation load was less intense, limiting canopy temperature and vapour pressure deficit.

Atmospheric CO_2 concentrations resulting from the fluxes discussed above exhibited a strong diurnal cycle (Fig. 5). The figure shows 'snapshots' of CO_2 during the second day of the cloud-free simulation. Just after sunrise (07:00 hours Fig. 5a), a layer of very high-concentration air was trapped under strong inversion, which was about 200 m deep. The air just above this stable layer exhibited much lower concentrations, with a CO_2 minimum at about 600 m above the forest. The relatively lower concentrations up to about 1.5 km altitude result from uptake during the previous day. This 'residual layer' of lower CO_2 is decoupled from the surface during the night because of the development of the stable layer near the surface, and would be subject to large-scale advection in the real world. The lateral boundaries for the model were periodic, however, so this residual layer has nowhere to go. By 09:00

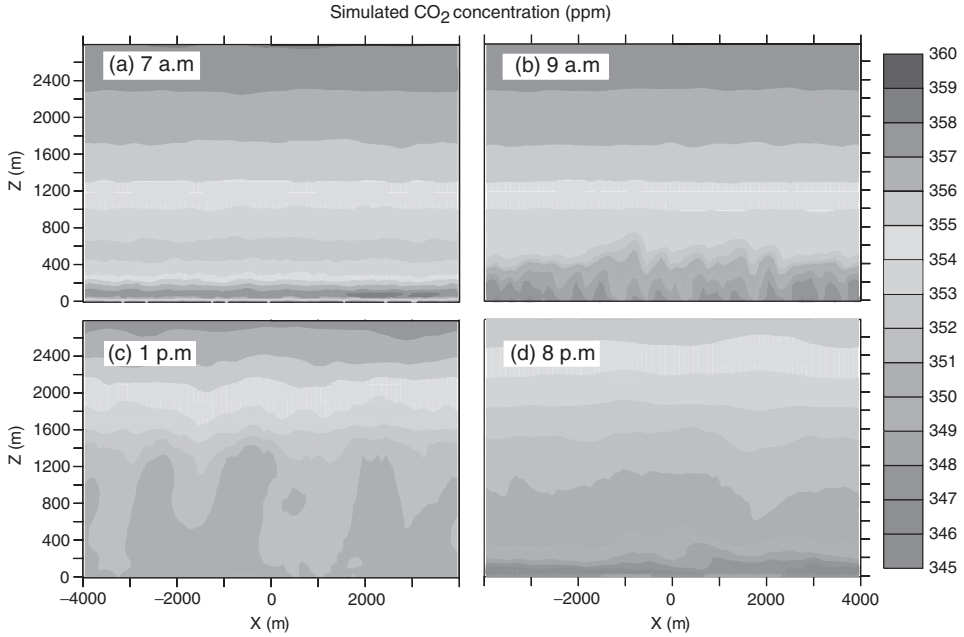

Fig. 5 Cross-sections of simulated CO_2 concentration in the lower troposphere: conditions at (a) 07:00 hours LST (b) 09:00 hours (c) 13:00 hours (d) 16:00 hours.

hours (Fig. 5b), the turbulent boundary layer had begun to grow into the residual layer, and photosynthesis was well underway. Entrainment of air into this growing PBL diluted the high-CO_2 air left over from the nocturnal stable layer. At the same time, photosynthesis was removing CO_2 from the still-shallow PBL, producing some of the lowest concentration values seen in the experiment. By 13:00 hours (Fig. 5c), the depth of the convective PBL had grown to about 1500 m, with relatively well-mixed CO_2 concentration. Gradients of 1–2 ppm resulted from convective updrafts rising from the forest with lower-than-average concentration and from downdrafts carrying above-average concentration air from the entrainment zone at the top of the PBL. Mid-day vertical gradients were extremely weak relative to the horizontal variability created by the large turbulent eddies. At 16:00 hours (Fig. 5d), a new stable layer had formed at the surface, resulting in the lowest CO_2 concentrations of the entire simulation because canopy activity had only recently ceased (discussed further below). The air above this low-CO_2 stable layer was decoupled from the surface due to the formation of the stable surface layer.

Qualitatively, the diurnal and vertical variations of the observed CO_2 concentration (Fig. 6a) show the same pattern as the simulation. The vertical gradient built up at night in the stable layer, with concentration differences of 80 ppm between the bottom and top of the tower developing by sunrise. As the turbulence grew deeper in the morning, this high-concentration air was diluted by entrainment from the residual layer, yet the growth of this layer led to a maximum concentration at 122 m about 2 h after the maximum at 30 m, and an hour later at 396 m. At mid-morning, the depth of the turbulence exceeded the top of the tower, and concentrations remained well-mixed for the rest of the day. Mid-day vertical gradients were weak, with about 2 ppm lower concentrations at the base than at the top of the tower. After sunset, with the cessation of photosynthesis roughly coinciding with the development of the stable layer, concentration gradients began to grow again, from the bottom-up.

Unlike the observations, the propagation of the morning maximum from the bottom to the top of the tower was minimal, with very little of the nocturnal buildup being expressed at the upper levels. This reflects the fact that photosynthesis depletes the surface stable layer more rapidly in the model than in the observations. Unlike the real atmosphere, by the time the simulated turbulence reached the upper levels of the tower, the accumulated CO_2 from nocturnal respiration had largely been consumed by the canopy. Maximum early morning concentrations at the 30 m level were slightly greater than observed. Another substantive difference between the simulations and the observations was in the concentrations just above the forest around sunset. Whereas the observations showed rising concentrations in the stable layer first at the

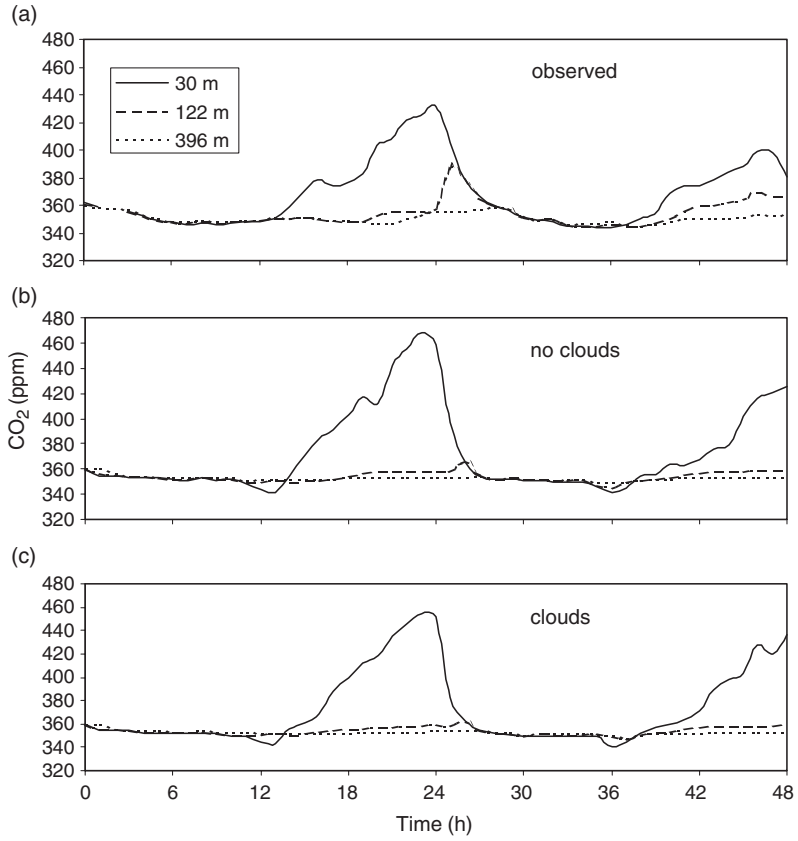

Fig. 6 Comparison of observed (a) and simulated CO_2 concentration at three levels on the WLEF-TV tower, without (b) and with (c) the presence of simulated clouds.

bottom of the tower, and later at mid-level, the simulations showed an evening minimum near sunset at the lowest level that was not observed.

Both morning and evening transitions involve rapid changes in photosynthesis, surface energy budget, and near-surface turbulence. Analysis of the evening transition (Fig. 7) revealed the mechanism behind the unobserved dip in concentration that occurred in the simulations. Latent heat flux (Fig. 7a) was consistently overestimated by the model, and persisted about an hour after canopy activity was observed to cease. Sensible heat flux (Fig. 7b) became negative at about 16:30 hours in the model when the simulated latent heat flux exceeded the net radiation, forming a very shallow stable layer near the surface. A very weak stable layer was in fact observed for this day, but it formed about an hour later than in the, model, and remained much less stable than the model until about 21:00 hours. Simulated CO_2 flux was also stronger than observed throughout the late afternoon, and the negative net ecosystem exchange continued until 19:00 hours (Fig. 7c). Actual NEE was observed to decrease gradually from about 13:00 hours and reach zero at about 18:00 hours. From about 16:30 hours until 19:00 hours, the model ecosystem was drawing CO_2 out of a very shallow stable layer, which prevented replenishment of CO_2 from the air aloft. The persistence of nearly mid-day levels of canopy activity (photosynthesis and transpiration) into the late afternoon is consistent with the multiyear offline simulations reported by Baker *et al.* (this issue), and probably results from over-estimation of canopy-averaged light-use efficiency in SiB. This caused the simulated CO_2 concentration (Fig. 7d) to decrease sharply just before sunset, reaching a minimum of 340 ppm, whereas the observed concentration was essentially constant through the period until it began to rise with the nearly simultaneous onset of positive NEE and negative sensible heat flux. Another contributing factor to the problems with simulating morning and evening transitions is the relatively coarse horizontal grid increment of 100 m. At this scale, smaller eddies associated with weak turbulence under low radiation conditions are not resolved. Apparently, the subgrid-scale turbulence scheme failed to represent properly the effect of these unresolved eddies, and led to stronger stratification than observed. Model sensitivity to subgrid-scale turbulence parameterizations was investigated by Nicholls *et al.* (2002), who found somewhat better simulation of vertical gradients using an alternative numerical scheme.

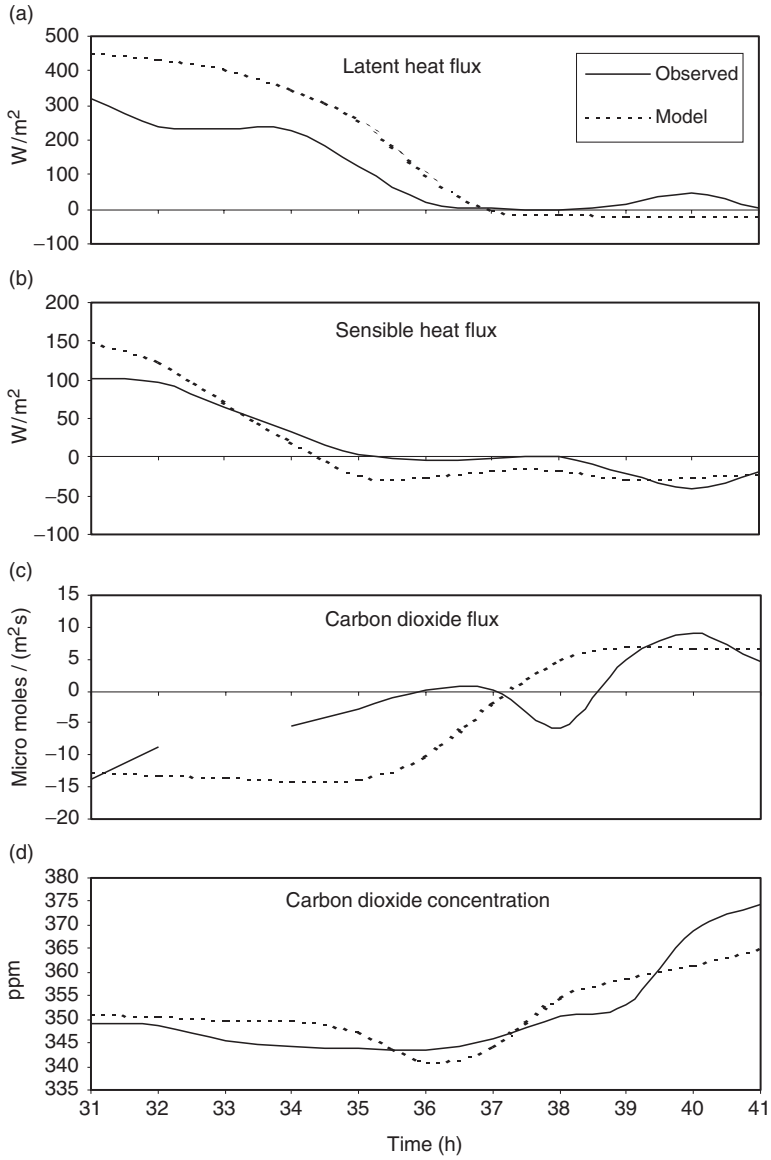

Fig. 7 Analysis of the evening transition on July 27, showing the early development of the stable layer in SiB-RAMS which was not observed. (a) Latent heat flux, (b) sensible heat flux, (c) carbon dioxide flux, and (d) carbon dioxide concentration at 30 m above ground. Time is elapsed time since the beginning of the experiment, in hours ($t = 31$ corresponds to 13:00 hours LST on July 27).

Conclusions

The coupled SiB2-RAMS model was reasonably successful in representing observed diurnal variations in fluxes of radiation, heat, water, and CO_2 at the WLEF tower site. Advantages of the coupled model relative to the offline simulations reported by Baker *et al.* (this issue) include the representation of the feedbacks between surface fluxes and PBL properties and the ability to compare simulated atmospheric CO_2 concentration to observations as an additional criterion for model evaluation. The diurnal cycle of the evolution of the PBL and the vertical profile of CO_2 in the high-resolution two-dimensional simulations is fairly consistent with the tower observations. The major exception is the development of a shallow CO_2 minimum in the simulations just before sunset. This arises because of a tendency of the model to overestimate late afternoon canopy activity (transpiration and photosynthesis), leading to persistent CO_2 uptake under a stable layer that forms about an hour too early. This phenomenon is attributed to misrepresentation of the extinction of direct beam radiation in SiB, resulting in overestimation of canopy-average light-use efficiency, and was also noted by Baker *et al.* (this issue). While the deviation of the simulated fluxes from the observations was fairly subtle, the effect on simulated CO_2 concentrations was obvious. This is an important advantage of the fully coupled simulations, and shows that prediction of an atmospheric scalar (CO_2) can in fact reveal subtle problems with the treatment of canopy biophysics.

Acknowledgements

This research was funded in part by the South-Central Regional Center (SCRC) of the National Institute for Global Environmental Change (NIGEC) through the US department of Energy (Cooperative Agreement No. DE-FC03-90ER61010, Contract No. TUL-106-00/01). Any opinions, findings and conclusions or recommendations expressed herein are those of the authors and do not necessarily reflect the view of the DOE. Support was also provided by COBRA (Contract No. ATM-982-1044) and by the US Department of Energy Contract DE-FG 03-02 ER 63474 A001.

References

Avissar R, Pielke RA (1991) The impact of plant stomatal control on mesoscale atmospheric circulations. *Agricultural and Forest Meteorology*, **54**, 353–372.

Baker I, Denning AS, Hanan N *et al*. (2001) Simulated and observed fluxes of sensible and latent heat and CO_2 at the WLEF-TV tower using SiB2.5. *Global Change Biology*, **9**, 1262–1278.

Bakwin PS, Tans PP, Hurst DF *et al*. (1998) Measurements of carbon dioxide on very tall towers: results of the NOAA/CMDL program. *Tellus*, **50B**, 401–415.

Ball JT (1988) An analysis of stomatal conductance. PhD Thesis, Stanford University, Stanford, California.

Charney J, Stone PH, Quirk WJ (1975) Drought in the Sahara: a biogeophysical feedback. *Science*, **187**, 434–435.

Collatz GJ, Ball JT, Grivet C *et al*. (1991) Physiological and environmental regulation of stomatal conductance, photosynthesis, and transpiration: a model that includes a laminar boundary layer. *Agriculture and Forest Meteorology*, **54**, 107–136.

Collatz GJ, Ribas-Carbo M, Berry JA (1992) Coupled photosynthesis-stomatal conductance model for leaves of C4 plants. *Australian Journal of Plant Physiology*, **19**, 519–538.

Davis KJ, Bakwin PS, Yi C *et al*. (2002) The annual cycles of CO_2 and H_2O exchange over a northern mixed forest as observed from a very tall tower. *Global Change Biology*, **9**, 1278–1293.

Deardorff JW (1980) Stratocumulus-capped mixed layers derived from a three-dimensional model. *Boundary Layer Met*, **18**, 495–527.

Denning AS, Collatz JG, Zhang C *et al*. (1996a) Simulations of terrestrial carbon metabolism and atmospheric CO_2 in a general circulation model. Part 1: surface carbon fluxes. *Tellus*, **48B**, 521–542.

Denning AS, Randall DA, Collatz GJ *et al*. (1996b) Simulations of terrestrial carbon metabolism and atmospheric CO_2 in a general circulation model. Part 2: spatial and temporal variations of atmospheric CO_2. *Tellus*, **48B**, 543–567.

Fan S-M, Gloor M, Mahlman J *et al*. (1998) A large terrestrial carbon sink in North America implied by atmospheric and oceanic carbon dioxide data and models. *Science*, **282**, 442–446.

Gurney KR, Law RM, Denning AS *et al*. (2002) Towards robust regional estimates of CO_2 sources and sinks using atmospheric transport models. *Nature*, **415**, 626–630.

Hansen MC, DeFries RS, Townshend JRG *et al*. (2000) Global land cover classification at 1 km spatial resolution using a classification tree approach. *International Journal of Remote Sensing*, **21**, 1331–1364.

Harrington JY (1997) The effects of radiative and microphysical processes on simulated warm and transition season Arctic stratus. PhD Dissertation, Colorado State University [Available from Colorado State University, Department of Atmospheric Science, Fort Collins, CO 80523.].

Holtslag AA, Boville BA (1993) Local versus non-local boundary-layer diffusion in a global climate model. *Journal of Climate*, **6**, 1825–1842.

Kalnay E, Kanamitsu M, Kistler R *et al*. (1996) The NCEP/NCAR 40-year reanalysis project. *Bulletin of the American Meteorological Society*, **77**, 437–471.

Los SO, Collatz GJ, Sellers PJ *et al*. (2000) A global 9-yr biophysical land surface dataset from NOAA AVHRR data. *Journal of Hydrometeorology*, **1**, 183–199.

Nicholls ME, Denning AS, Prihodko L *et al*. (2002) A multiple-scale simulation of variations in atmospheric carbon dioxide using a coupled biosphere-atmospheric model. *Journal of Geophysical Research* (in press).

Nicholls ME, Pielke RA (2000) Thermally induced compression waves and gravity waves generated by convective storms. *Journal of Atmospheric Science*, **57**, 3251–3271.

Nicholls MERA, Pielke JL, Eastman CA *et al*. (1995) Applications of the RAMS numerical model to dispersion ver urban areas. In: *Wind Climate in Cities* (eds Cermak JE *et al*.), pp. 703–732. Kluwer Academic Publishers, Dordrecht, The Netherlands.

Nicholls ME, Pielke RA, Meroney RN (1993) Large eddy simulation of microburst winds flowing around a building. *Journal of Wind Engineering and Industrial Aerodynamics*, **46847**, 229–237.

Pielke RA (1974) A three-dimensional numerical model of the sea breezes over south *Florida Monthly Weather Review*, **102**, 115–139.

Pielke RA, Avissar R, Raupach M *et al*. (1998) Interactions between the atmosphere and terrestrial ecosystems: influence on weather and climate. *Global Change Biology*, **4**, 101–115.

Pielke RA, Cotton WR, Walko RL *et al*. (1992) A comprehensive meteorological modelling system RAMS. *Meteorology and Atmospheric Physics*, **49**, 69–91.

Rayner PJ, Enting IG, Francey RJ *et al*. (1999) Reconstructing the recent carbon cycle from atmospheric CO_2 $\delta^{13}C$ and O_2/N_2 observations. *Tellus*, **51B**, 213–232.

Sarmiento JL, Wofsy SC, Shea E *et al*. (1999) A carbon cycle science plan. Interagency Working Group Report, US Climate and Global Change Research Program.

Schaefer K, Denning AS, Suits N *et al*. (2002) The effect of climate on inter-annual variability of terrestrial CO_2 fluxes. *Global Biogeochemical Cycles*, **16**, 1102–1029.

Sellers PJ, Heiser MD, Hall FG (1992) Relations between surface conductance and spectral vegetation indices at intermediate ($100\,m^2$ to $15\,km^2$) length scales. *Journal of Geophysics Research*, **97**, 19033–19059.

Sellers PJ, Los SO, Tucker CJ *et al*. (1996b) A Revised Land-Surface Parameterization (SiB2) for Atmospheric GCMs. Part 2: The generation of global fields of terrestrial biophysical parameters from satellite data. *Journal of Climate*, **9**, 706–737.

Sellers PJ, Mintz Y, Sud YC *et al*. (1986) A simple biosphere model (SiB) for use within general circulation models. *Journal of Atmospheric Science*, **43**, 505–531.

Sellers PJ, Randall DA, Collatz GJ *et al*. (1996a) A revised land-surface parameterization (SiB2) for atmospheric GCMs. Part 1: Model formulation. *Journal of Climate*, **1**, 676–705.

Shukla J, Mintz Y (1982) Influence of land-surface evapotranspiration on the earth's climate. *Science*, **215**, 1498–1501.

Soil Survey Staff (1994) *State Soil Geographic Database (statsgo)*. US Department of Agriculture, Natural Resources, Conservation Service, Fort Worth, TX.

Teillet PM, El Saleous N, Hansen MC *et al*. (2000) An evaluation of the global 1-Km AVHRR land dataset. *International Journal of Remote Sensing*, **21**, 1987–2021.

Tripoli GJ, Cotton WR (1981) The use of ice-liquid water potential temperature as a thermodynamic variable in deep atmospheric models. *Monthly Weather Review*, **109**, 1094–1102.

Tripoli GJ, Cotton WR (1982) The Colorado State University three-dimensional cloud/mesoscale model – 1982. Part I: General theoretical framework and sensitivity experiments. *Journal De Recherche Atmosphére*, **16**, 185–220.

Walko RL, Cotton WR, Harrington JL *et al*. (1995b) New RAMS cloud microphysics parameterization Part I: The single-moment scheme. *Atmospheric Research*, **38**, 29–621.

Walko RL, Tremback CJ, Pielke RA *et al*. (1995a) An interactive nesting algorithm for stretched grids and variable nesting ratios. *Journal of Applied Meteorology*, **34**, 994–999.